EasyChair Preprint

№ 6932

Thermal Characteristics of Biogas Flameless Combustion in Asymmetric Meso-scale Combustor

Ali Asmayou, Mazlan Abdul Wahid and
Mohammed Bashir Abdulrahman

October 26, 2021

Thermal Characteristics of Biogas Flameless Combustion in Asymmetric Meso-scale Combustor

Ali Houssein Asmayou[1], Mazlan Abdul Wahid[1], Mohammed Bashir Abdulrahman[1]

[1] *High-Speed Reacting Flow Laboratory, Faculty of Engineering, School of Mechanical Engineering, Universiti Teknologi Malaysia, 81310 UTM Skudai, Johor, Malaysia.*

. Corresponding author: [a)] alihasmayou@gmail.com
[b)] mazlan@utm.my
[c)] *mobash2007@gmail.com*

Abstract. Thermal characteristics of non-premixed conventional flame and flameless mode at fixed fuel mass flow rate of biogas (60% CH4 + 40% CO2) in an asymmetric meso-scale vortex combustor. Axial and tangential oxidizer configurations are investigated in this paper. The three-dimensional form of governing equations including the Realizable-k–e model and the eddy-dissipation have been described using to simulate temperature distribution and combustion stability. The effect of tangential oxidizer configurations on the temperature distribution is also explored. The non-premixed meso-scale flameless combustion is much more stable compared to the non-premixed conventional flame. With a low of 10 % O2 concentration, the meso-scale flameless mode has higher temperature homogeneity throughout the combustor than conventional flame. The maximum temperature in meso-scale non-premixed conventional flame and flameless combustions were 1692 K and 1160 K respectively.

Keywords: Meso scale combustion, Flameless mode, Non-Premixed, Biogas, tangential air

INTRODUCTION

The miniaturization of small-size power supply systems with high energy density is becoming a significant topic in nowadays world. The demand for compact, lightweight power has motivated researchers to actively dwell in designing a small reacting system. In a meso-scale combustor, the length scale ranges from 1 mm to 10 cm for power generation of 10 W to 1 kW. Because of the high ratio of the surface zone to volume, there is higher surface heat loss in the meso-scale combustor and this can extinguish reactions to oblige flame unstable. Restricted flow residence time is likewise another issue to be contemplated with respect the flame stability. [1–5]. However, the reduction of size in the combustion system has encountered some technical challenges. This study has also been motivated by the speedy development of meso-scale electrical mechanical systems, during the last few decades. Combustion plays a significant role in this regard because it is particular power obstetrics when the shift efficiency and performance from thermal energy to electrical energy is considered. The most advanced currently available lithium batteries have an energy density of 1.2 MJ/kg. Thus, a small combustion appliance with only 3% system efficiency could compete with the batteries. Utilizing the high specific energy of liquid hydrocarbon fuels in combustion-driven micro-appliances for generating power was proposed by several researchers[6,7]. Along with the demands for further developments of small-scale combustion devices, fundamentals on micro and meso-scale combustion also collect increasing interests through the technical challenge to overcome quenching issues due to the large surface-to-volume ratio of small-scale devices[8]. Flameless combustion is a recently improved combustion system, which gives near-zero-emission production. Flameless combustion has several advantages over conventional combustion. Flameless combustion is characterized by having temperature distribution uniformity, which originates from the dispersed reaction zone and is accompanied by a relatively small increase in temperature as a result of the dilution of combustion air or fuel with flue gases or inert gas before combustion. The uniform temperature inside the combustion chamber confirms homogeneously mixed reactor conditions. Since the peak of temperature decreases in the flameless process and hot stains vanishes, NO_x formations minimize drastically[6,9–11] Multiple efforts have been stated, as well as frequent ongoing efforts, to overcome this challenge and achieve consistent heat generation in micro/meso-scale combustors.[12]. Biogas is considered a promising candidate for renewable energy[13]. It's composed primarily of methane and carbon dioxide, with a little carbon monoxide (CO), hydrogen sulfide (H2S), and siloxanes[14]. Palm oil mill effluent (POME) is a major source of biogas in Malaysia[15]. Methane (50–70%) and carbon dioxide (30–50%) are the main components of biogas produced by anaerobic digestion[16]. The low calorific value (LCV) of biogas is about 30 MJ/kg,60% CH_4[17]. The high CO_2 content in biogas reduces the methane-air mixture's low flame speed, which is approximately 40 cm/s. The methane autoignition temperature at about 640 ◦C, while the biogas autoignition temperature at about 700 ◦C[13]. Because of these considerations, biogas must be purified, or a better combustor design must be applied[16]. In this study, an asymmetric a meso-scale vortex combustor has been developed to work under flameless mode using biogas as fuel with the long-term aim to produce moderate power at high efficiency and low level of emissions.

COMBUSTOR CONFIGURATION

Fig. 1 shows a schematic of the asymmetric meso-scale combustion chamber. This concept has ten configurations for air and three configurations for fuel. The position of air jets that is perpendicular with fuel jets would enhance vortex flow in the combustor chamber or other words such as vortex is created by the introduction of the air with a full tangential velocity component to the asymmetric combustor. The essence of the present tangential configurations offering a swirl component in the central zone of the combustor, along with axial fuel flow. This device consists of a vertical combustion chamber with a radius of 10 mm with offset radius displacement of 2.88 and thick 35 mm developed by a refractory cement cylinder to reduce heat loss to surroundings, meanwhile preserving temperatures inside the chamber is greater than the auto-ignition of the fuel and covered from outside by a stainless-steel cover with a thickness of 15 mm. Each half of the cylinder includes three distributed inlets for tangential airflow with a radius of 1.5 mm, two inlets for axial fuel flow with a radius of 1.44 mm and the length of the combustion chamber is 55 mm. The position of fuel and air inlets is eclectically configured to allow the correct mixing of air and fuel inside the strong field of forced vortexes. Such swirling is generated by interjecting the air with a whole tangential velocity component axial to the combustor. The gases are extricated at the other end of the meso-scale vortex flameless combustion chamber through a circular hole. Two cases of air configurations were chosen for this study, axial and reverse have 6 inlets and tangential has 4 inlets.

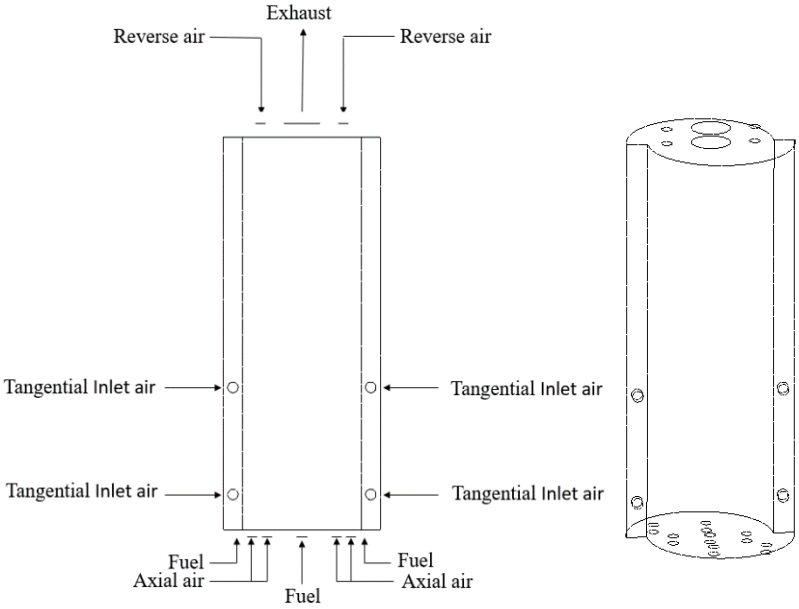

FIGURE 1. Schematic of the asymmetric Meso-Scale combustion

COMPUTATIONAL APPROACH

ANSYS workbench fluent 19.0 based on the finite element method with a three-dimensional solver was applied to discretize the flow domain through a second-order upwind scheme (more precise than the first order), to guarantee the grid independence of the solution, numerous tetrahedron grids were generated. The SIMPLE algorithm was employed to obtain the mass conservation, in the discretized momentum equation, between the pressure and velocity terms. The chemical reaction was recognized as a volumetric kind and the Eddy Dissipation Model (EDM) algorithm was selected for turbulence chemistry interactions. It is noticeable to indicate here that EDM is the only known combustion model that is eligible for simulating non-premixed (i.e. at the inlet) flames that have more than one fuel inlet, which is the case for the asymmetric vortex flames[18–20]. Fig 2 shows the geometry of the asymmetric meso-scale combustion. The implementation temperature and pressure were 300K and 100Kpa respectively. The partial equilibrium model was used to predict the O radical concentration required for thermal No prediction. A steady-state pressure-based solver was utilized, in the whole of the simulations, to solve the governing equations through the CFD code. The situation in which the solution converged was when the residuals were less than $1\times10{-}4$ at consecutive iterations. Moreover, the solution for the chemical reactions equation and energy equation converged at quantities less than $1\times10{-}7$. The flow domain variables, on the above-mentioned conditions, reached stable local values regarding any number of iterations. Further, monitoring for parameters of NOx and temperature converged independently, too. The specifics of boundary conditions, which were simulated in this study to investigate the meso-scale vortex flameless characteristics, are shown in Table 1.

FIGURE 2. The geometry of the asymmetric Meso-Scale combustion

TABLE 1. Boundary condition of simulation

Turbulence Model	Realizable K-epsilon		
Reaction Model	Volumetric reaction, Species Transport reaction with Eddy Dissipation of turbulence chemistry model, methane air two step		
Inlet and Boundary Conditions	Air Inlet	Velocity(flame)	7.7 m/sec
		Velocity(flameless)	17 m/sec
		Temperature	300 K
		Flame Concentration (mole fraction)	O_2 =21%, N_2 = 79%
		Flameless Concentration (mole fraction)	O_2 =10%, N_2 = 90%
	Fuel Inlet	Velocity(flame)	1.5 m/sec
		Velocity(flameless)	4.9 m/sec
		Temperature	300 K
		Biogas Concentration	60% CH_4, 40%CO_2
		Material	refractory cement
	Wall	Ambient temperature	300 K

GRID INDEPENDENT CHECK

The convenient terminology for describing the enhancement of results using successively smaller cell sizes for the calculations is 'Grid convergence' as the mesh becomes finer; a calculation should approach the correct answer. The normal CFD technique should start with a coarse mesh and slowly refine it until the changes which are observed in the results are smaller than a pre-defined acceptable error. A grid independence test was performed to evaluate the effects of grid sizes on the results as shown in Figure 3. Four sets of mesh were generated using tetrahedron elements with M1 = 2,208 nodes, M2 = 18,797 nodes, M3 = 68,250 nodes, and M4 = 164,552 nodes. It was perceived that the M3 = 68,250 nodes and M4 = 164,552 nodes produce nearly identical results along with the chamber with a few average percentage errors Hence, a domain with M3 = 68,250 nodes was chosen to reduce the computing time. The computational domain of the vortex combustor is shown in Figure 4.

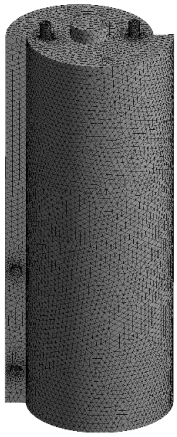

FIGURE 3. Mesh of the asymmetric meso-scale combustion

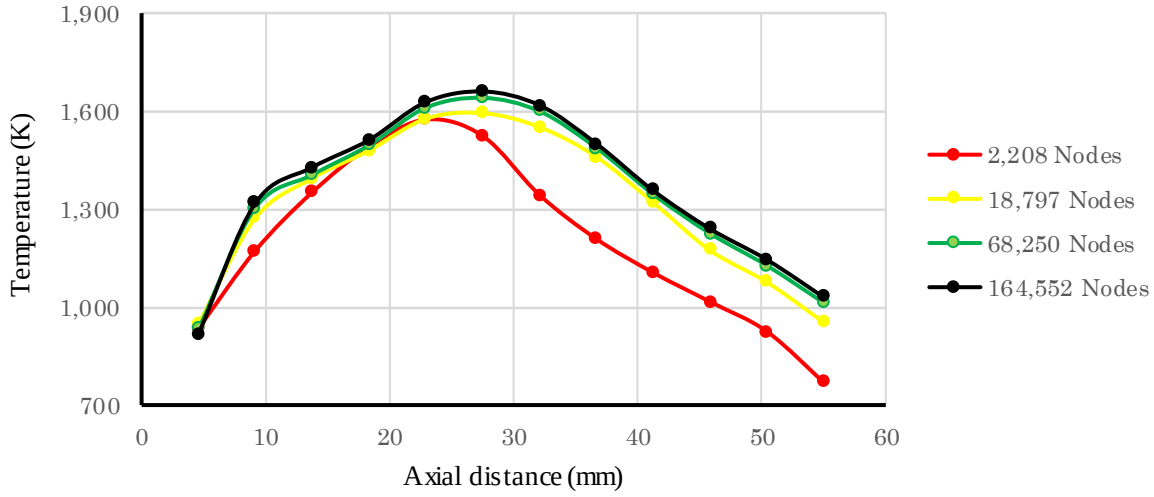

FIGURE 4. Grid independence test

RESULTS AND DISCUSSION

At this stage of work, the pattern of temperature is presented at center planes to observe thermal characteristics of the meso-scale combustor, through increasing the mass flow rate and with the different oxygen concentrations and same equivalent ratio. The result from Figure 5 shows that two different cases of air case(a) reverse and axial configurations, case(b) tangential configurations. The result in case (a), shows that the flame temperature gathered in the middle of the combustion chamber, due to the axial and reverse air inlets. Case (b), showing that the flame temperature was distributed throughout the combustion chamber and this is due to the tangential air inlets that create a vortex field as shown in figures 5,6. The vortex field caused by the tangential air intake is important for mixing in the chemical reaction during the combustion process. In case (a), the highest flame temperature was recorded at 1692 K before half the distance of the combustion chamber, while in case of (b) the highest flame temperature was recorded at 1640 K after the middle of the axial distance of the furnace. Meanwhile, in cases (a, b), the temperature was uniform and distributed in flameless mode compared to traditional flame.

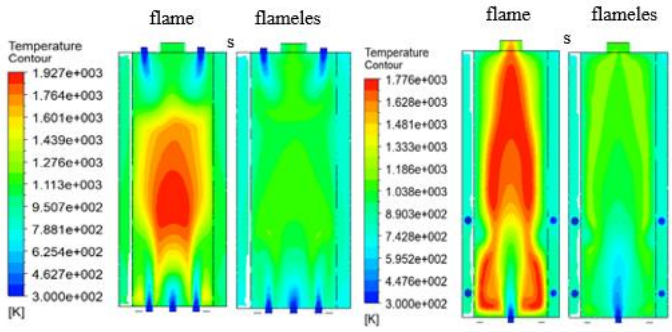

Case (a) Case (b)

FIGURE 5. Effect of axial configurations Case (a) and tangential Case (b) on the temperature distribution for the conventional combustion and flameless combustion at the center of the ZX-plane.

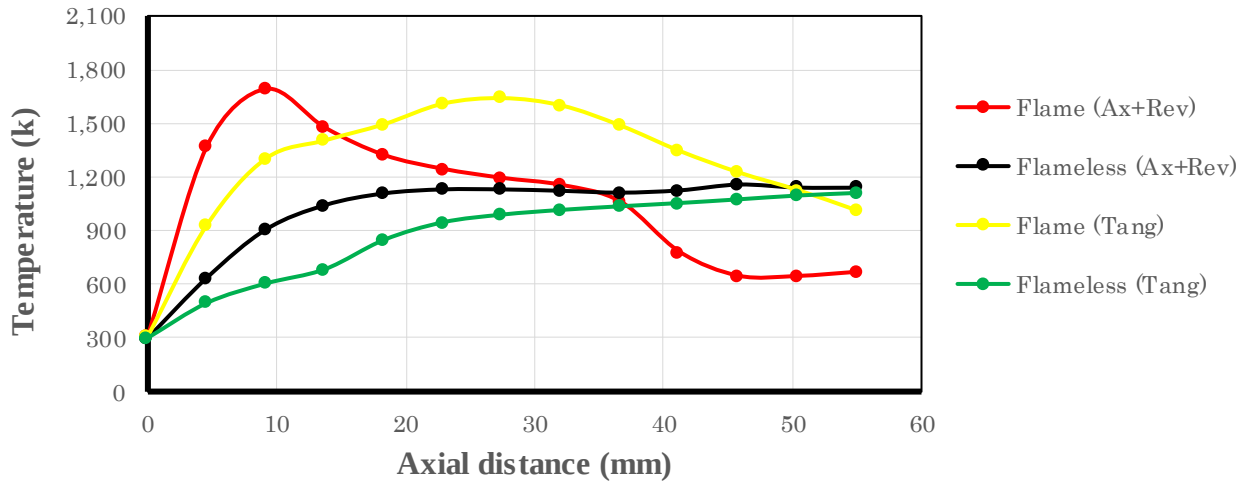

FIGURE 6. The combustion chamber temperature as a function of axial distance for conventional and flameless mode for two cases.

CONCLUSION

In this work, a computational study (ANSYS) of Thermal Characteristics of meso-scale flameless combustion has been done and the characteristic of this technology has been obtained involve a uniform thermal domain in a meso-scale combustion chamber. The model of combustor geometry, oxygen concentration, and the method of mixing fuel and air affect temperature distribution. A vast range of computational techniques has been done to show the predictions of the combustor characteristics and to investigate the itemized flow evolution. In the combustor volume considered in this study, the stable flame and flameless were achieved at stoichiometric equivalence ratio for hydrocarbon fuel (biogas). Comparison between the flame and flameless mode through two cases of various inlets configurations were investigated. The case of tangential air configuration was more temperature uniform than axial and reverse air configuration.

.

References

1. T.T. Leach, C.P. Cadou, The role of structural heat exchange and heat loss in the design of efficient silicon micro-combustors, Proc. Combust. Inst. 30 II (2005) 2437–2444. https://doi.org/10.1016/j.proci.2004.08.229.
2. Y. Ju, B. Xu, Theoretical and experimental studies on mesoscale flame propagation and extinction, Proc. Combust. Inst. 30 II (2005) 2445–2453. https://doi.org/10.1016/j.proci.2004.08.234.
3. D.G. Norton, D.G. Vlachos, Hydrogen assisted self-ignition of propane/air mixtures in catalytic microburners, Proc. Combust. Inst. 30 (2005) 2473–2480. https://doi.org/10.1016/j.proci.2004.08.188.
4 G.A. Boyarko, C.J. Sung, S.J. Schneider, Catalyzed combustion of hydrogen-oxygen in platinum tubes for micro-propulsion applications, Proc. Combust. Inst. 30 (2005) 2481–2488. https://doi.org/10.1016/j.proci.2004.08.203.
5. S. Karagiannidis, J. Mantzaras, G. Jackson, K. Boulouchos, Hetero-/homogeneous combustion and stability maps in methane-fueled catalytic microreactors, Proc. Combust. Inst. 31 II (2007) 3309–3317. https://doi.org/10.1016/j.proci.2006.07.121.
6. D.C. Walther, J. Ahn, Advances and challenges in the development of power-generation systems at small scales, Prog.

Energy Combust. Sci. 37 (2011) 583–610. https://doi.org/10.1016/j.pecs.2010.12.002.
7. A.C. Fernandez-Pello, Micropower generation using combustion: Issues and approaches, Proc. Combust. Inst. 29 (2002) 883–899. https://doi.org/10.1016/s1540-7489(02)80113-4.
8. K. Maruta, Micro and mesoscale combustion, Proc. Combust. Inst. 33 (2011) 125–150. .https://doi.org/10.1016/j.proci.2010.09.005.
9. S. Komonhirun, P. Yongyingsakthavorn, U. Nontakeaw, Effects of mesh type on a non-premixed model in a flameless combustion simulation, 2018. https://doi.org/10.1088/1757-899X/297/1/012071.
10. A.A.A. Abuelnuor, M.A. Wahid, H.A. Mohammed, A. Saat, Flameless combustion role in the mitigation of NOX emission : a review, (2014) 827–846. https://doi.org/10.1002/er.
11. J.A. Wünning, J.G. Wünning, Flameless oxidation to reduce thermal no-formation, 1997. https://doi.org/10.1016/s0360-1285(97)00006-3.
12. S. Wu, S. Abubakar, Y. Li, ScienceDirect Thermal performance improvement of premixed hydrogen / air fueled cylindrical micro-combustor using a preheater-conductor plate, Int. J. Hydrogen Energy. (2020). https://doi.org/10.1016/j.ijhydene.2020.10.237.
13. M.M. Sies, M.A. Wahid, Numerical investigation of the asymmetrical vortex combustor running on biogas, J. Adv. Res. Fluid Mech. Therm. Sci. 74 (2020) 1–18. https://doi.org/10.37934/ARFMTS.74.1.118.
14. E.I. Ohimain, S.C. Izah, A review of biogas production from palm oil mill effluents using different configurations of bioreactors, Renew. Sustain. Energy Rev. 70 (2017) 242–253. https://doi.org/10.1016/j.rser.2016.11.221.
15. M.Z. Alam, N.A. Hanid, Development of indigenous biofilm for enhanced biogas production from palm oil mill effluent, J. Adv. Res. Fluid Mech. Therm. Sci. 39 (2017) 1–8.
16. M. Persson, O. Jonsson, A. Wellinger, Biogas Upgrading To Vehicle Fuel Standards and Grid, IEA Bioenergy. (2007) 1–32.
17. A. Noyola, J.M. Morgan-Sagastume, J.E. López-Hernández, Treatment of biogas produced in anaerobic reactors for domestic wastewater: Odor control and energy/resource recovery, Rev. Environ. Sci. Biotechnol. 5 (2006) 93–114. https://doi.org/10.1007/s11157-005-2754-6.
18. R.A. ALWAN, A, THERMAL AND FLUID FLOW ANALYSIS OF SWIRLING FLAMELESS COMBUSTION, BMC Public Health. 5 (2017) 1–8. https://ejournal.poltektegal.ac.id/index.php/siklus/article/view/298%0Ahttp://repositorio.unan.edu.ni/2986/1/5624.pdf%0Ahttp://dx.doi.org/10.1016/j.jana.2015.10.005%0Ahttp://www.biomedcentral.com/1471-2458/12/58%0Ahttp://ovidsp.ovid.com/ovidweb.cgi?T=JS&P.
19. K.M. Saqr, Turbulent Vortex Flames: Aerodynamics and Thermochemistry of Turbulent Confined Vortex Flames, Universiti Teknologi Malaysia, 2011. http://www.amazon.com/Turbulent-Vortex-Flames-Aerodynamics-Thermochemistry/dp/3846546224.
20. M. Khaleghi, S.E. Hosseini, M.A. Wahid, H.A. Mohammed, The Effects of Air Preheating and Fuel/Air Inlet Diameter on the Characteristics of Vortex Flame, J. Energy. 2015 (2015) 1–10. https://doi.org/10.1155/2015/397219.